

Performance of nonwoven geotextile-reinforced walls under wetting conditions: laboratory and field investigations

F. H. M. Portelinha¹, B. S. Bueno² and J. G. Zornberg³

¹Associate Professor, Federal University of São Carlos, Civil Engineering Department – DECiv, Rodovia Washington Luis, km 235, mailbox 676, São Carlos, São Paulo, 13.565-905, Brazil, Telephone: +55 16 3351 82 62, Telefax: +551633518262, E-mail: fportelinha@ufscar.br

²Titular Professor, School of Engineering of University of São Paulo at São Carlos, University of São Paulo, Geotechnical Engineering Department, Trabalhador São-carlense avenue 400, São Carlos, São Paulo, 13.566-536, Brazil, Telephone: +55 16 3373 95 01, Telefax: +55 16 3373 95 09, E-mail: bsbueno@sc.usp.br

³Fluor Centennial Professor, The University of Texas at Austin, Civil Engineering Department – GEO, 1 University Station C1792 Austin, TX 78712-0280, USA, Telephone: +1 303 492 04 92, Telefax: +1 512 471 65 48, E-mail: zornberg@mail.utexas.edu

Received 29 August 2012, revised 10 January 2013, accepted 14 January 2013

ABSTRACT: The first geosynthetic retaining wall in Brazil was constructed in 1984 as an instrumented 10 m high geotextile-reinforced soil wall with a poorly draining backfill. This structure has been showing excellent performance throughout its service life, even after long periods of rainfall. In the past, the excellent performance of the wall had been attributed to the influence of soil confinement on the geotextile strength properties as well as the comparatively high interface shear strength between the fine soil and the nonwoven geotextile. Now there is also evidence of the beneficial effect of the internal drainage capacity when using nonwoven geotextiles as reinforcements. In order to clarify the understanding of the performance of the pioneer history case wall (SP-123 wall) and the effect of nonwoven geotextiles as reinforcements of fine-grained soils, full-scale laboratory models of geotextile reinforced walls were tested under wetting conditions. Results from the instrumentation have shown no significant positive water pressures and relatively small displacements even after intense periods of precipitation. The consistency between field and laboratory investigations provides strong evidence in support of the use of nonwoven geotextiles to reinforce poorly draining soils.

KEYWORDS: Geosynthetics, Geotextile, Wetting, Reinforced soil wall

REFERENCE: Portelinha, F. H. M., Bueno, B. S. & Zornberg, J. G. (2013). Performance of nonwoven geotextile-reinforced walls under wetting conditions: laboratory and field investigations. *Geosynthetics International*, 20, No. 2, 90–104. [<http://dx.doi.org/10.1680/gein.13.00004>]

1. INTRODUCTION

Although granular soils are recommended in design of geosynthetic-reinforced soil (GRS) structures in North America (Elias and Christopher 1998; AASHTO 2002) and Europe (BSI 1995), geosynthetic-reinforced soil walls have often been constructed with on-site native soils. Use of these soils (often poorly draining soils) leads to cost savings in areas where granular materials are difficult to procure (Zornberg and Mitchell 1994; Stulgis 2005; Pathak and Alfaro 2010). However, the use of backfill soils capable of developing positive pore water pressures may result in some serviceability problems (e.g. excessive deformations) or failures of reinforced soil walls (Mitchell

and Zornberg 1995; Stulgis 2005; Yoo and Jung 2006). Koerner and Soong (2001) present a survey describing 12 walls with serviceability problems and 14 wall failures, which included a total of 17 walls constructed using poorly draining soils as backfill.

Recently, the frequency of rain-triggered landslides around the world has been increasing, coincident with the effects of climate change. In this regard, structural mitigation measures through the application of geosynthetics have been exploited in localities where rain-triggered landslides are a potential threat to human life and property (Fowze *et al.* 2012). A number of studies have reported excellent performance of geosynthetic-reinforced walls constructed

using poorly draining backfill, even when subjected to long periods of rainfall (Carvalho *et al.* 1986; Tatsuoka and Yamauchi 1986; Mitchell and Zornberg 1995; Benjamin *et al.* 2007). A common aspect of these projects has been the use of nonwoven geotextiles to reinforce fine-grained soils. In fact, the hydraulic properties of nonwoven geotextile reinforcements can be useful in dissipating pore water pressures and, consequently, enhancing the internal stability of the structure (Fourie and Fabian 1987; Ling *et al.* 1993; Zornberg and Mitchell 1994; Tan *et al.* 2001; Iryo and Rowe 2005; Noorzad and Mirmoradi 2010; Raisinghani and Viswanadham 2010, 2011). The reinforcement layers provide internal drainage, increasing the drainage capacity of the backfill. Tan *et al.* (2001) have reported that nonwoven geotextile reinforcements provide an internal drainage capacity three times higher than that of unreinforced backfill. Permeability experiments conducted by Raisinghani and Viswanadham (2010) have shown that the use of a nonwoven geosynthetic layer as a drainage element for marginal soils enhances the equivalent in-plane permeability of a soil–geosynthetic system. This encourages its possible use in enhancing the pore-water pressure dissipation for geosynthetic-reinforced slopes and walls constructed with marginal soils.

Furthermore, the intrusion of soil particles into the pores of nonwoven geotextile and the soil confinement have been reported to significantly improve the tensile strength and the creep behaviour of the reinforcement (Mendes and Palmeira 2008; França and Bueno 2011). However, clogging of nonwoven geotextiles and the existence of wet soil conditions along soil–geosynthetic interfaces can inhibit performance as a drainage system (Raisinghani and Viswanadham 2010).

This paper includes an evaluation of nonwoven geotextile-reinforced walls constructed with fine-grained soil under wetting conditions in order to observe the effect of the hydraulic properties of nonwoven geotextiles on the performance of GRS walls. The evaluation included a laboratory instrumented full-scale model subjected to rainfall events. The models allowed assessment of the mechanical response of the reinforcements as well as the hydraulic performance of the wall under rainfall events. A case history involving the performance of a nonwoven geotextile-reinforced wall is reported, illustrating the general field behaviour of nonwoven geotextiles used to reinforce a poorly draining soil. Finally, a comparative assessment of field and laboratory responses is presented.

2. PERFORMANCE OF A PIONEER GEOTEXTILE-REINFORCED WALL

The first geosynthetic-reinforced wall in Brazil was constructed in 1984 and involved a reinforced steep slope with a facing inclination of 1H:2V. The structure was designed to rebuild a slope failure approximately 30 m high, in the SP-123 Roadway, state of São Paulo, Brazil. Figure 1 shows the wall during construction. The reinforced wall is 10 m high, with a front facing of 500 m², constructed over a 10 m high compacted soil embankment. Another compacted embankment was constructed over the reinforced

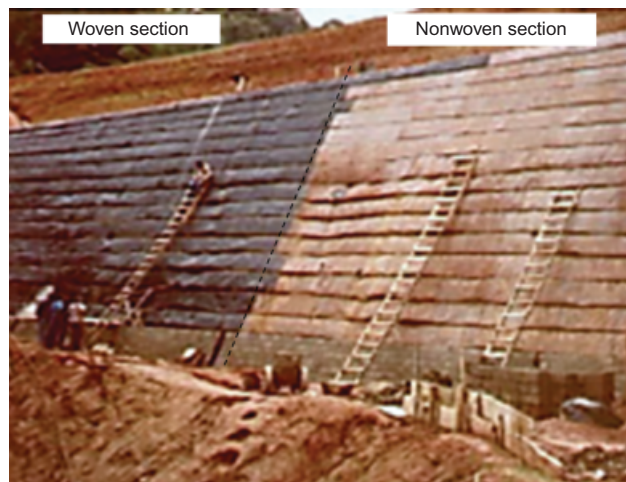


Figure 1. A view of the SP-123 wall, a pioneer geosynthetic-reinforced wall in Brazil

wall, reaching the total of 30 m high (Figure 2a). A polypropylene woven geotextile (167 g/m²) and a needle-punched polyester nonwoven geotextile (300 g/m²) were used as reinforcements in different sections. Both reinforced sections had a vertical spacing of 0.60 m (Figure 2b). Both geotextiles have an ultimate tensile unconfined strength of 22 kN/m, with elongations at the failure of 10% and 39% for the woven and nonwoven geotextiles, respectively (Ehrlich *et al.* 1997). The internal drainage system includes face drains, while the surface water control comprises concrete drainage channels on the top and at the toe of the wall. Precast concrete blocks were used to form the wraparound facing. The structure was instrumented (Figure 2b) in order to monitor its performance and to establish the need for mitigation action in case of serviceability problems.

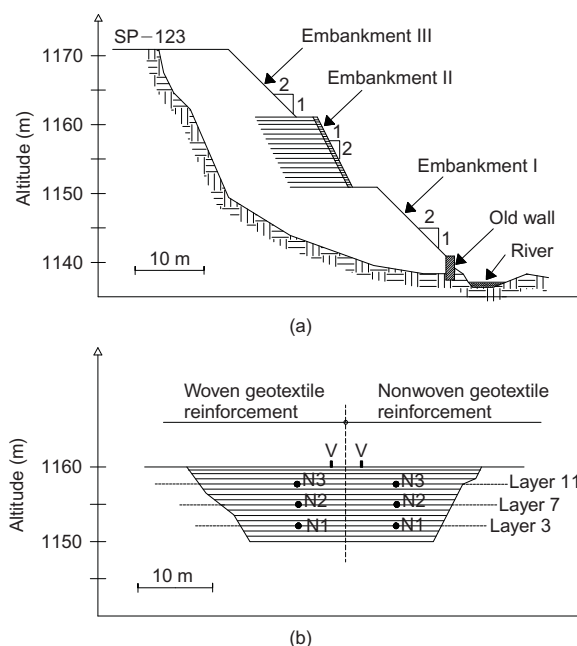


Figure 2. Geotextile-reinforced wall: (a) cross-section; (b) front view and location of instrumentation (Vidal *et al.* 1990)

The backfill material is a clayey silt sand (granite residual soil) with a liquid limit of 44% and a plasticity index (PI) of 14%, maximum dry unit weight of 16.7 kN/m³ and optimum water content of 16.8%. Results from direct shear tests have shown cohesion of 22 kPa and a friction angle of 35° (Vidal *et al.* 1990; Ehrlich *et al.* 1997). According to Federal Highway Administration recommendations for mechanically stabilised earth walls (Elias and Christopher 1998), the backfill soil gradation (5% clay, 21% silt, 68% sand, 6% gravel) would not meet specifications for soil fines contents exceeding 15%.

Precipitation data are relevant for assessing the possible wetting of the backfill soils. Average monthly precipitation (based on records collected over 68 years) is pre-

sented in Figure 3. In addition, the specific monthly precipitation recorded in the years 1984 to 1986 (periods of construction and instrumentation monitoring) is also shown in the figure. A long period of rainfall is observed from October to March, indicating periods of intense precipitation during construction. Periods of high precipitation occurred during the lifetime of the wall, so wetting into the backfill is expected.

Monitoring of the wall was conducted using piezometers, earth pressure cells, horizontal mechanical extensometers and vertical magnetic extensometers. Instrumentation design and records were reported by Carvalho *et al.* (1986) and by Ehrlich *et al.* (1997). The instrumentation was installed in three reinforced layers: the 3rd, 7th and 11th layers from the base of the wall, as indicated in Figure 2b. Instrument readings were taken during construction and the two initial years of serviceability. Instrument locations within each monitored layer are shown in Figure 4. Earth pressure cells were installed in the 3rd and 11th reinforced layers, accessing vertical and horizontal stresses. Internal displacements were monitored using extensometers located at 1, 3 and 6 m from the facing. A piezometer was installed in the third layer within the nonwoven geotextile section. Vertical magnetic extensometers were placed in all instrumented layers. Instrumentation results are presented in Figure 5.

Instrumentation data shows that a significant proportion of the horizontal movements occurred during the construction phase. It should be noted that construction occurred during the wettest period of 1984. As a result, horizontal displacements in the woven geotextile section were larger

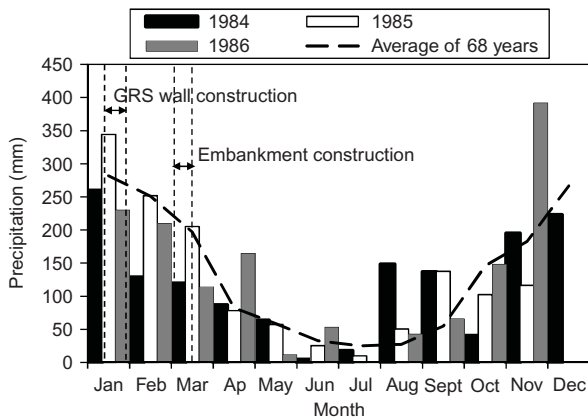


Figure 3. Precipitation in the vicinity of the SP-123 wall

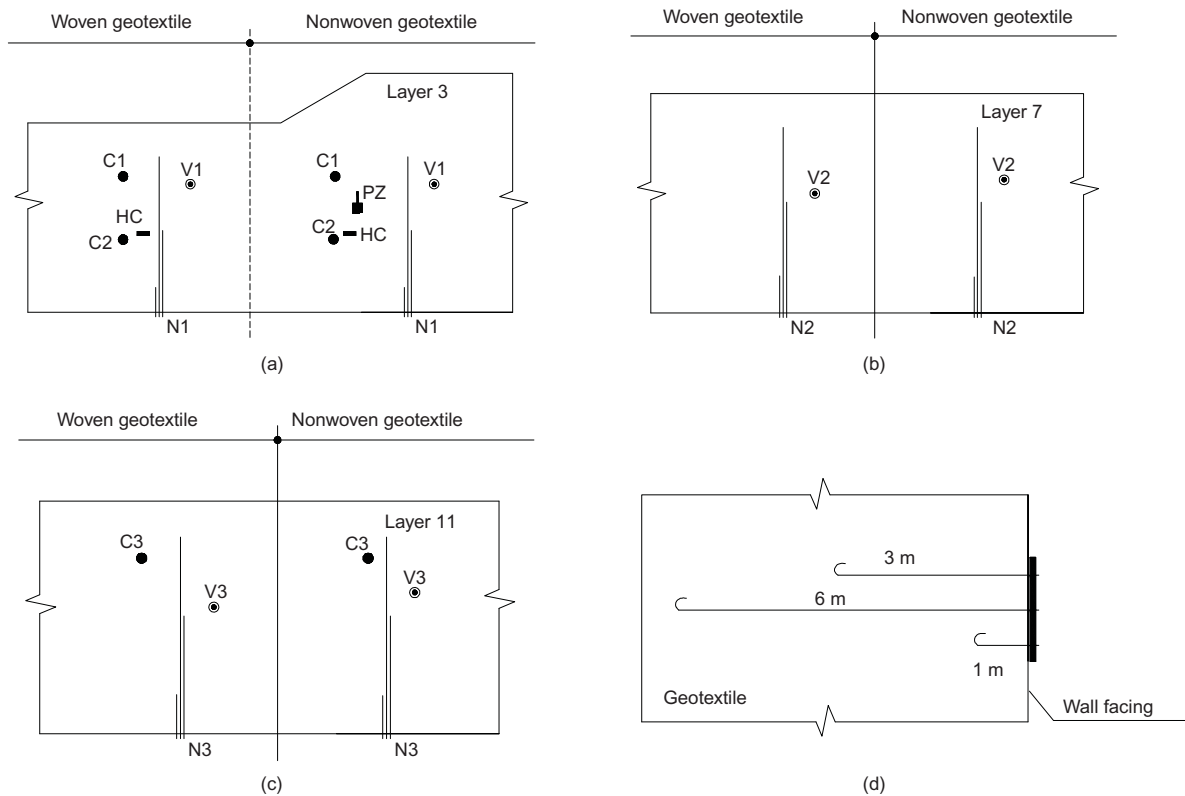


Figure 4. Instrument locations of the SP-123 wall: (a) layer 3; (b) layer 7; (c) layer 11; (d) horizontal extensometers. C, vertical pressure cells; HC, horizontal pressure cells; N, extensometers; PZ, piezometers; V, settlement plates (Vidal *et al.* 1990)

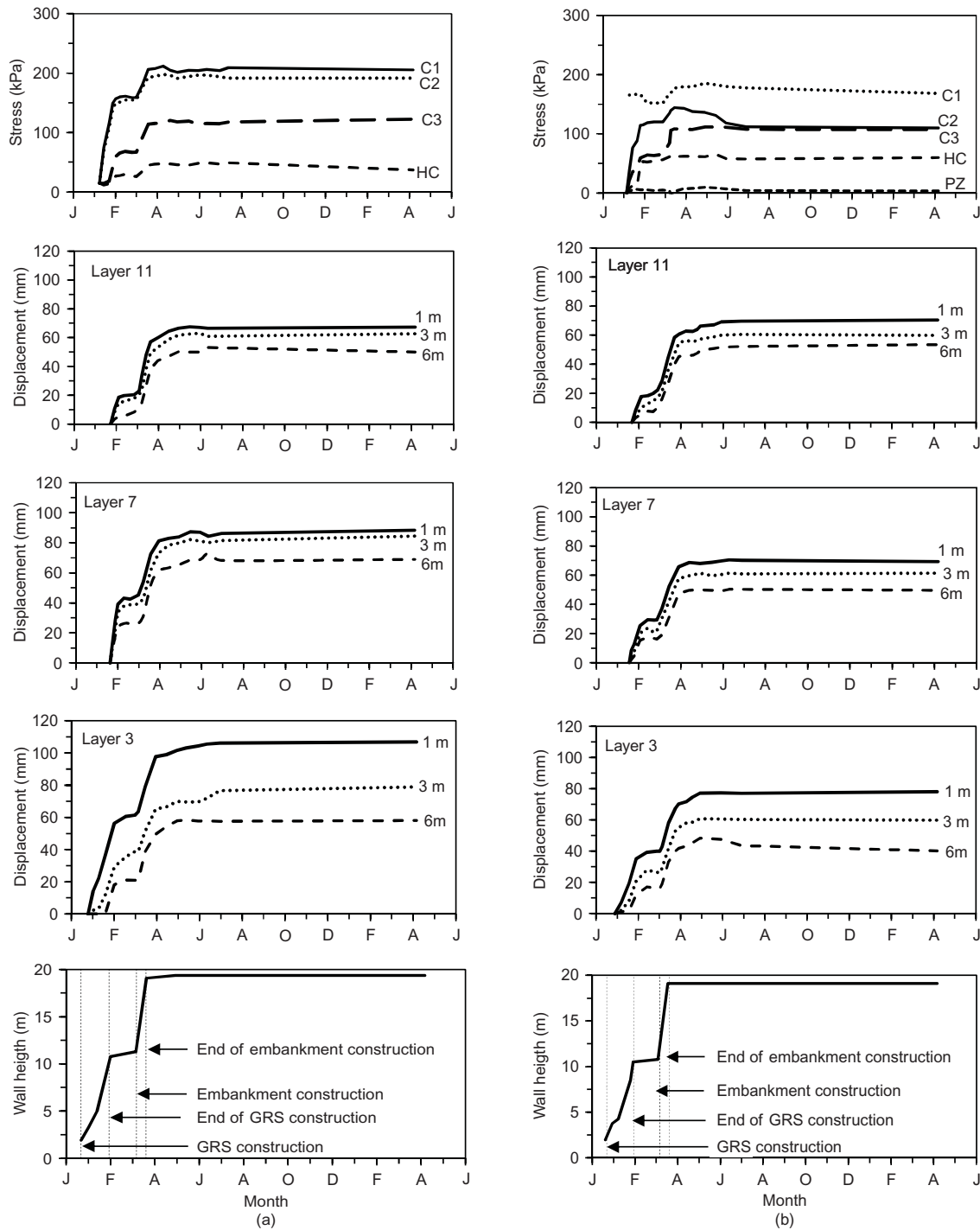


Figure 5. Performance of the SP-123 wall: (a) woven geotextile section; (b) nonwoven geotextile section (redrawn after Vidal *et al.* (1990))

than in the nonwoven geotextile section. Specifically, the maximum relative horizontal displacements (normalised to wall height) were 1.2% and 0.6% for the woven and nonwoven sections, respectively. Overall, the magnitudes of movements were comparatively small and, also, time-dependent displacements were negligible. Additionally, the piezometers showed either negative or comparatively small (positive) pore water pressures in the nonwoven geotextile section during the 2 years of monitoring.

A field investigation was recently conducted of the moisture conditions of the backfill soil in this structure based on samples collected in July 2010. The field work

involved extractions of soil samples from different locations within the reinforced zone (2.0 m from the face). The gravimetric water content results are presented in the schematic front view of the wall in Figure 6.

The recently obtained water content results are significantly higher than the compaction water content, which confirms that the backfill has been subjected to wetting. Another important observation is that the water content values observed in the nonwoven geotextile section are lower than those observed in the woven geotextile section. This provides evidence of the drainage capacity of nonwoven geotextiles.

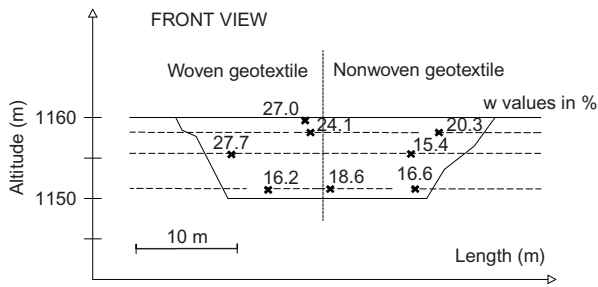


Figure 6. Water contents of backfill after 26 years of service for nonwoven and woven sections of the SP-123 wall

The SP-123 wall investigation also included visual condition analysis and survey monitoring. Figure 7 illustrates some of the wall’s features after 26 years of service. The face showed good condition, although short-root vegetation had developed on the facing surface, as shown in Figure 7a. No cracks were noted on the concrete block facing, implying that wall distortion was insignificant. The concrete drainage channels at the toe and crest of the structure remained in good condition (Figure 7b). Surveying conducted by the Department of Roadways and High-

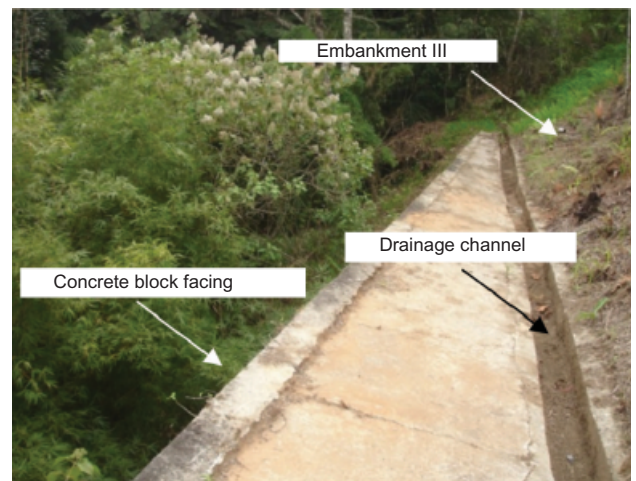
ways of Brazil (DER) indicated insignificant changes in the facing inclination since 1986 for the nonwoven section, but an increased facing inclination was noted in the woven section, as indicated in Figure 8.

Internal stability analyses were conducted to provide an indication of the wall stability using the AASHTO simplified method (AASHTO 2002) and, comparatively, a limit equilibrium analysis (Wright and Duncan 1991) indicating the geotextile-stabilised forces. All the limit equilibrium analyses shown herein were conducted with circular slip surface and Spencer’s procedure (Spencer 1967).

For both analyses the soil strength parameters from direct shear tests and the ultimate tensile strength of geotextiles were used, as previously indicated. Both analyses were conducted to assess breakage failure stability, while pullout stability analyses were negligible. AASHTO simplified methods indicated the failure of this structure with a minimum safety factor of 0.5. Nowadays, reinforcements with strength properties as in the case of the pioneer reinforced wall would not be applied, for safety reasons. However, limit equilibrium analyses have resulted in a factor of safety of 1.85 with the failure surface shown in Figure 8. Regarding the development of



(a)



(b)



(c)



(d)

Figure 7. Current state of the SP-123 wall: (a) facing view; (b) top view; (c) lateral view; (d) upper part view

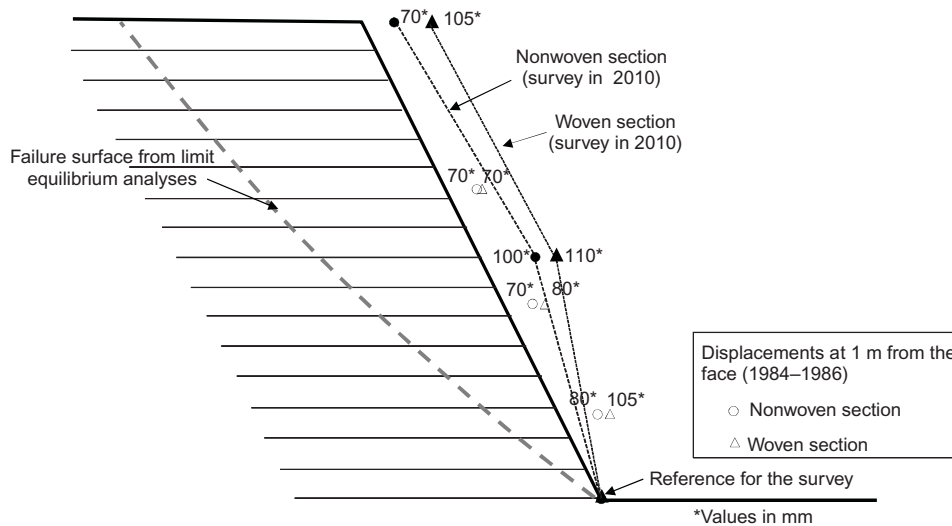


Figure 8. Face displacements of the case history wall between 1984 and 1986 (Ehrlich *et al.* 1997) and during a recent investigation in 2010

pore water pressure, the structure would fail with 30 kPa of pore water pressure. Concerning the likelihood of development of pore water pressure during the structure’s life or during the construction process, the case history design can be considered high risk.

3. PERFORMANCE OF A PROTOTYPE GEOTEXTILE-REINFORCED WALL

3.1. Overview

Full-scale prototype walls were constructed at the Geosynthetics Laboratory of the São Carlos School of Engineering at the University of São Paulo, Brazil. A strong metallic box container was used to house prototype reinforced soil wall structures, which were 1.8 m high and 1.55 m wide, with backfill soil extending to a distance of 1.8 m from the front edge of the box. The structure was seated on a rigid concrete foundation. The soil is laterally contained by two parallel metallic counterfort walls bolted to the structural floor of the laboratory. The box includes a metallic lid that is bolted to the lateral walls, constituting a stress reaction structure. The lid confines an air bag used to apply a uniform surcharge to the soil surface. A uniform surcharge pressure of up to 200 kPa can be applied to the structure. The back of the reinforced fill is also restrained by a metallic wall. The inside surfaces of the metallic box were lubricated with petroleum jelly and covered with polyethylene sheeting to facilitate the development of plane strain conditions.

3.2. Materials

The fine soil used to construct the full-scale prototype is a clayey sand with a hydraulic conductivity of 4.9×10^{-7} m/s. Physical properties of the soil included a G_s of 2.751, maximum dry unit weight of 17.88 kN/m³, w_{opt} of 14.6%, w_L of 39.7%, w_p of 20.3%, and PI of 19.4%. A comparison of the particle size distributions of the soil used in this prototype and in the case history is presented in Figure 9. This indicates that both soils are composed of practically

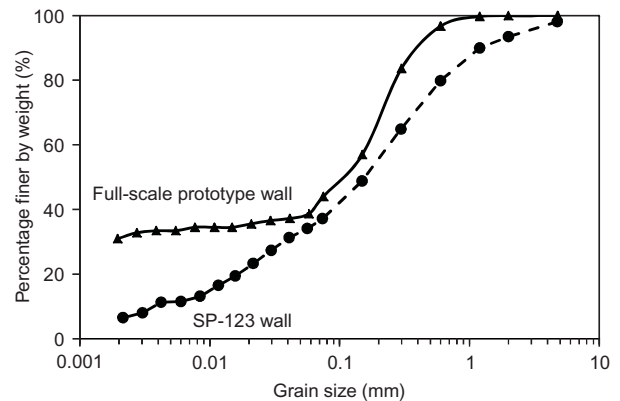


Figure 9. Particle size distribution of the full-scale prototype and SP-123 wall backfills

40% of fine particles. As in the case history, this soil would also not meet the AASHTO (2002) specifications. The shear strength of the soil, evaluated by consolidated drained (CD) triaxial compression tests, resulted in a friction angle of 32° and cohesion of 15 kPa.

A needle-punched polyester nonwoven geotextile was used as reinforcement. The nonwoven geotextile had thickness of 2.69 mm (NBR 12569 1992), mass per unit area of 293 g/m² (NBR 12568 1992), and wide-width tensile strength and elongation at failure (in the longitudinal direction) of 10 kN/m and 83%, respectively (ASTM D 4595). A relatively weak and extensible geotextile was specifically selected for the prototype wall in order to generate measurable strains.

3.3. Full-scale prototype wall

Two reinforced-soil prototype walls were constructed (Figure 10). The soil was compacted to 98% relative density (in relation to the maximum dry unit weight from the standard Proctor test) and optimum water content. The optimum water content was achieved by mixing the water into soil and equilibrating before it was compacted in the box test.



(a)



(b)

Figure 10. Full-scale prototype wall: (a) wraparound exposed facing during construction; (b) under working conditions

In order to achieve the required density relative, layers of 5 cm height were manually compacted. Compaction control was achieved using the drive-cylinder method (ASTM D 2937) in each of the 30 cm high compacted layers. Geotextile reinforcements were placed at 30 cm vertical spacing with slope of 1% towards the face. Each reinforcement layer had a total length of 1.80 m, measured from the face. A typical cross-section is presented in the Figure 11. The wall was constructed with a wraparound facing and no batter. Protective shotcrete coating ranging from 5 to 8 cm was used to reproduce actual working conditions. Drainage geocomposites were used as face drainage elements across the shotcrete in the second and fourth reinforced layers as indicated in Figure 11.

3.4. Wetting system

After construction, a wetting system was installed on the top of the wall surface, which was prepared to have an inclination of 2% toward the face. This wetting system is composed by supplying pipes and a water distribution layer seated on the top of the structure. The water distribution layer includes a 15 cm high sand layer and a drainage geocomposite installed over the sand layer. The configuration of the drainage geocomposite and the sand layer allowed a uniform water distribution on the top surface. Water was supplied by a reservoir with a float switch enabling constant hydraulic load and assuring constant rainfall intensity. The intensities of precipitation were regulated for manual measurements of volumetric flow rate in the output water tap installed in the water reservoir, using a bucket and chronometer. Figure 12 shows features of the wetting system.

3.5. Instrumentation

Instrumentation was installed to monitor pore water pressures, soil water content, internal horizontal displacements,

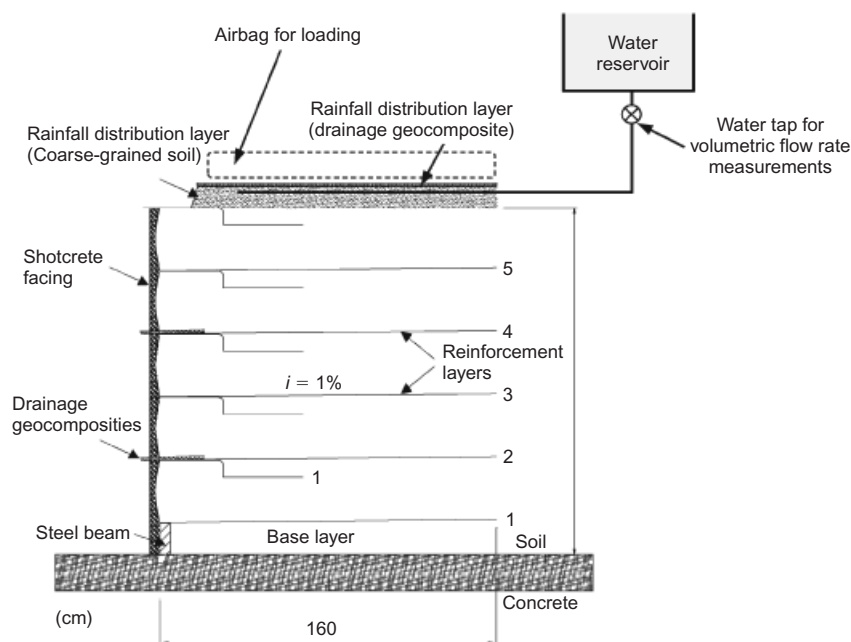


Figure 11. Cross-section view of the full-scale prototype

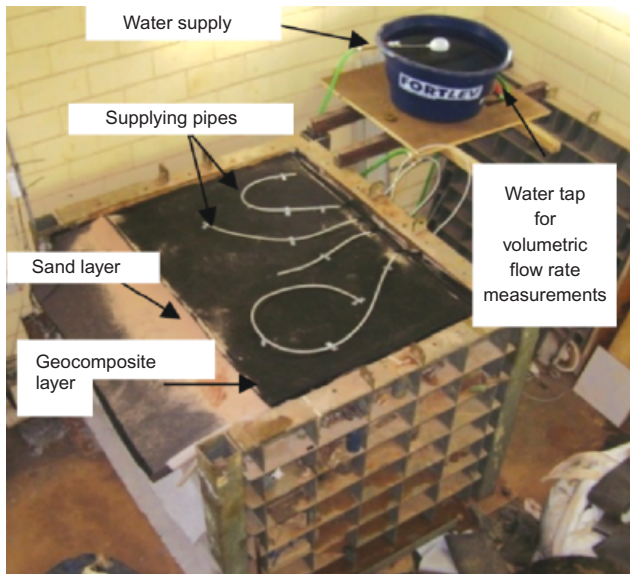


Figure 12. Wetting system

ments, reinforcement strains and horizontal face displacements. The instruments layout is presented in Figure 13.

The infiltration of water into the model was monitored using piezometers with a measurement range of -100 to 100 kPa, placed at the middle of each reinforced layer as well as 5 cm above the reinforcements. Frequency domain reflection (FDR) sensors were installed to measure the water contents in each reinforced layer (located 10 cm above the reinforcement).

Internal displacements were measured by mechanical extensometers (tell-tales). This device consists of stainless steel inextensible wires that run inside tubes used to reduce friction and to protect the wires. One end of the tell-tales is fixed to the geotextile and the opposite is connected to a small weight used to tension the wires and to obtain measurements of relative displacement. Measurements were made using a digital caliper with a resolution of 0.01 mm. Tell-tales were fixed at five points distributed along each reinforcement layer (spaced every 30 cm) as shown in Figure 13. They allowed the internal displacements to be obtained at different points of each reinforcement layer, covering its entire length. The horizontal face displacements of the wall were measured using dial

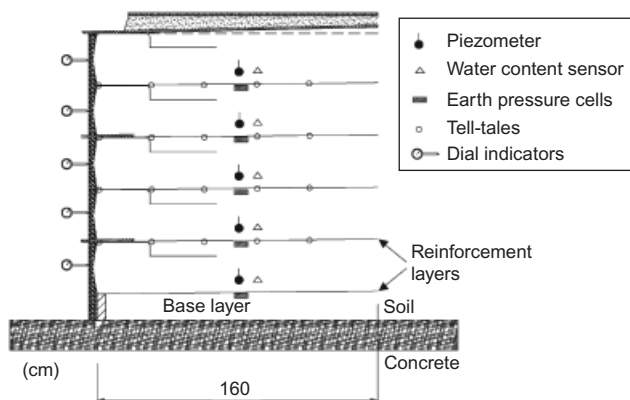


Figure 13. Instrument locations of the full-scale prototype

indicators located at the center of each reinforced layer (Figure 13).

3.6. Prototype simulations

The simulation procedure consisted of the recording of instrumentation results of two full-scale models under rainfalls events and loading. The setup allowed rainfall and loading to occur simultaneously. Figure 14 summarises the rainfall events intensities and durations, which were selected to reproduce actual precipitation in field conditions. In prototype 1, medium intensities were applied with comparatively short drying periods. For prototype 2, high intensities of rainfall were reproduced, but with long drying periods. These rainfall patterns were selected in order to observe the water pressure behaviour in the reinforced zone, as well as the role of geotextiles in dissipating internal pressures. Figure 15 shows the loading regime in prototypes 1 and 2. In prototype 1, the increment of loading was chosen in order to trigger the build-up of positive pore water pressures within the reinforced zone.

4. SIMULATION RESULTS

4.1. Performance under working conditions: prototype 1

Figure 16 presents the effect of water infiltration on the degree of saturation and the pore water pressure in

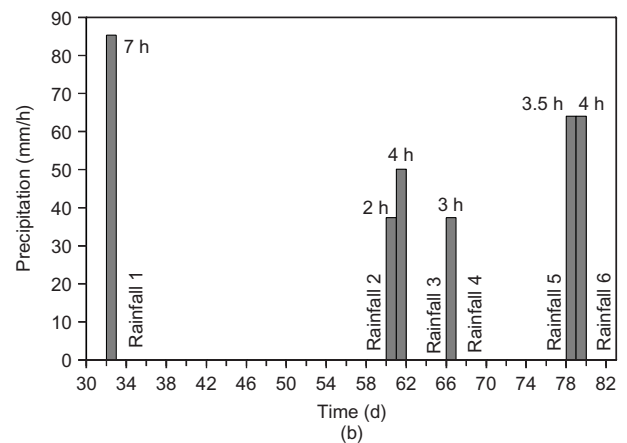
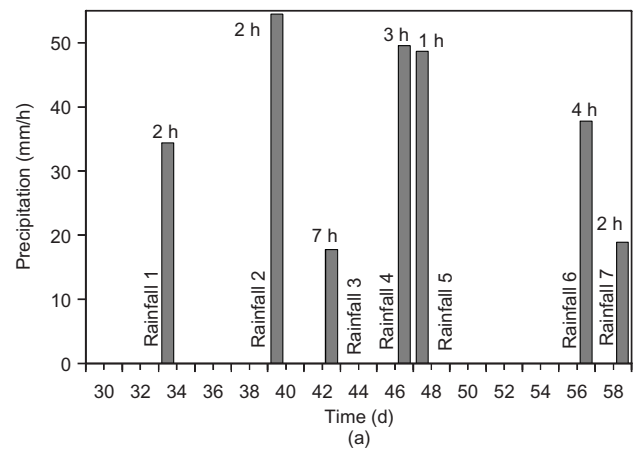


Figure 14. Rainfall intensities: (a) prototype 1; (b) prototype 2

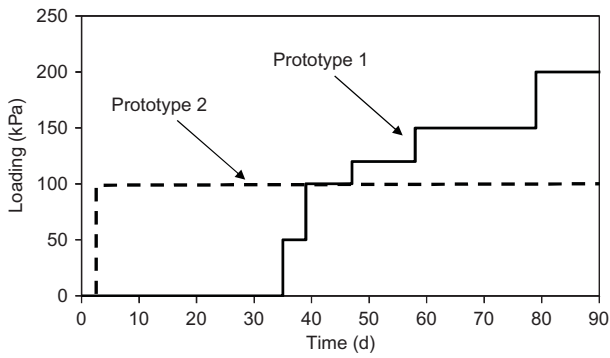


Figure 15. Loading regime of prototypes 1 and 2

prototype 1. Clearly, the precipitation led to a wetting front that advanced downwards into the reinforced zone, resulting in maximum values of degree of saturation of approximately 90%. In general, the degree of saturation is comparatively smaller in lower layers, providing evidence of the contribution of the draining reinforcements in the upper layers. Piezometer readings indicated that positive water pressures did not develop during the test, providing further evidence of water pressure dissipation along the geotextile layers.

Figure 17 presents the internal displacements in each reinforced layer of prototype 1, as measured at the facing

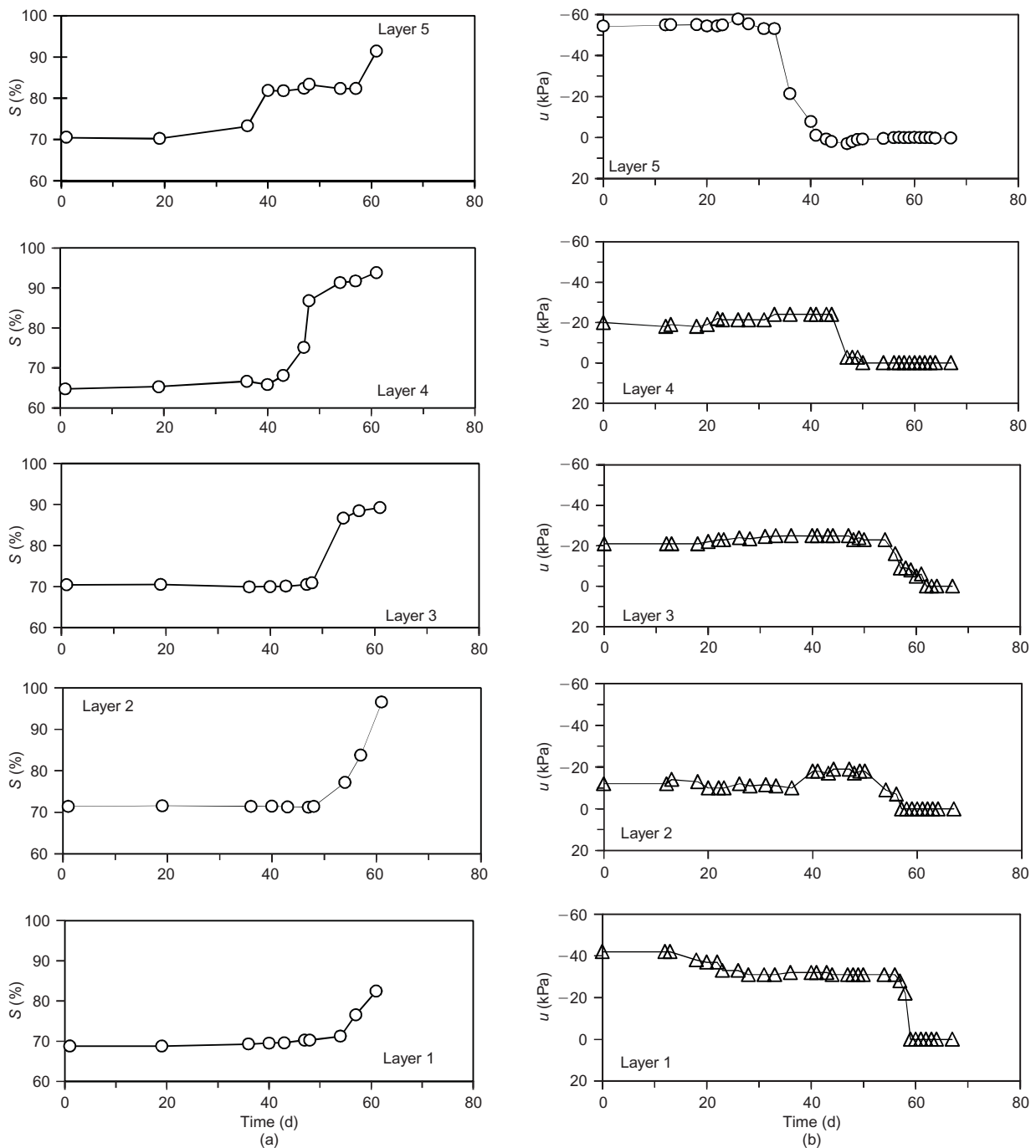


Figure 16. (a) Degree of saturation S and (b) pore water pressure u measurements in prototype 1

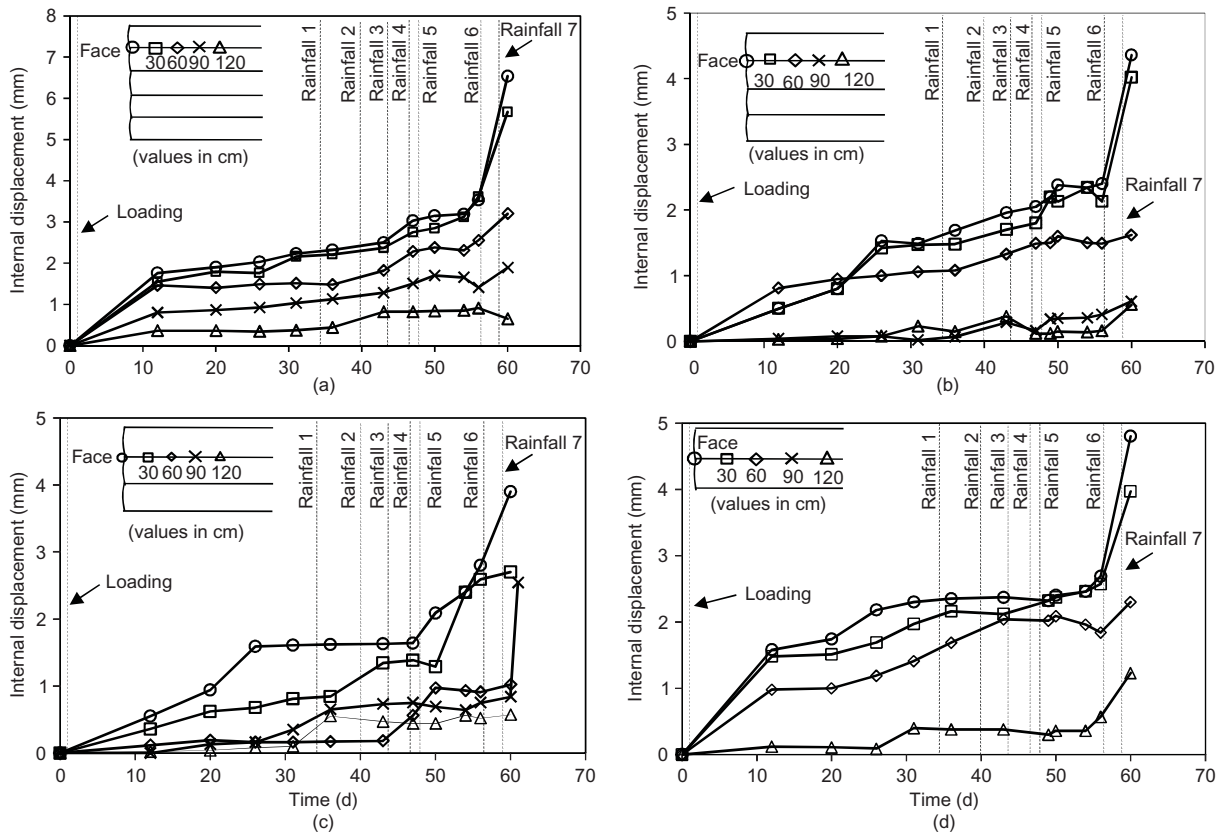


Figure 17. Horizontal internal displacements in prototype 1: (a) layer 5, (b) layer 4, (c) layer 3; (d) layer 2

and at 30, 60, 90 and 120 cm from the facing of the wall. In general, displacements were relatively small during the test (maximum of 6 mm), although they increased progressively during the wetting process. The progressive reduction of soil stiffness caused by the wetting advancement is assumed to have led to the displacements in the wall. As a result, higher displacements occurred after the wetting front reached the toe. In other words, additional displacements occurred when the soil suction was progressively reduced along the failure surface.

Reinforcement strains were computed using information collected on the relative horizontal displacements between the face and points of tell-tale fixation along reinforcement layers (Figure 13). The distribution of relative displacements along one of the reinforcement layers of prototype 1 is presented in Figure 18. In this figure, sigmoidal curves were defined to fit the raw displacement data in order to have a smooth representation of the distribution of displacements along the reinforcement length. This displacement function can then be used to obtain the distribution of strains along the reinforcement length, as presented by Zornberg and Arriaga (2003). Geotextile strains are often obtained by calculating the relative movements between consecutive mechanical extensometers (tell-tales) and dividing them by the initial distance between points of measurement. However, this technique often leads to significant scatter, particularly if the distance between measured points is significant. Consequently, the raw data from extensometer displacement was initially smoothed by fitting the data to a sigmoidal curve and the distribution of strains along the geotextile

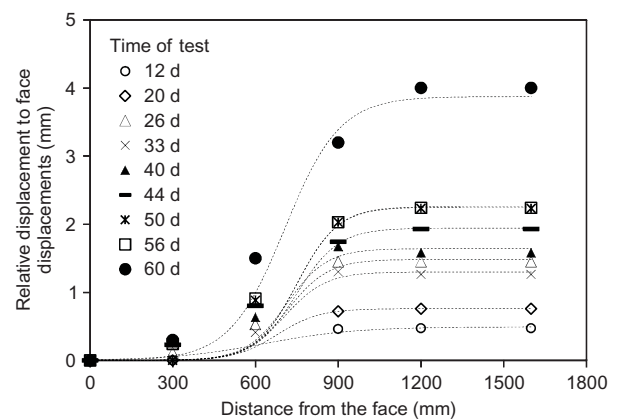


Figure 18. Displacement distributions along the reinforcement 4 in prototype 1

length was obtained by differentiating the displacement function as

$$\epsilon = d\left(\frac{1}{a + be^{-cx}}\right) / dx \quad (1)$$

where d is the extensometer displacement, x is the distance from the face to the measured point, and a , b and c are parameters defined by fitting a sigmoidal curve to the raw data using the least-squares technique.

The strain distributions and the location of peak of strains on the reinforcements of prototype 1 are shown in Figure 19. The potential failure plane defined by the locus of the maximum reinforcement strains, the critical failure

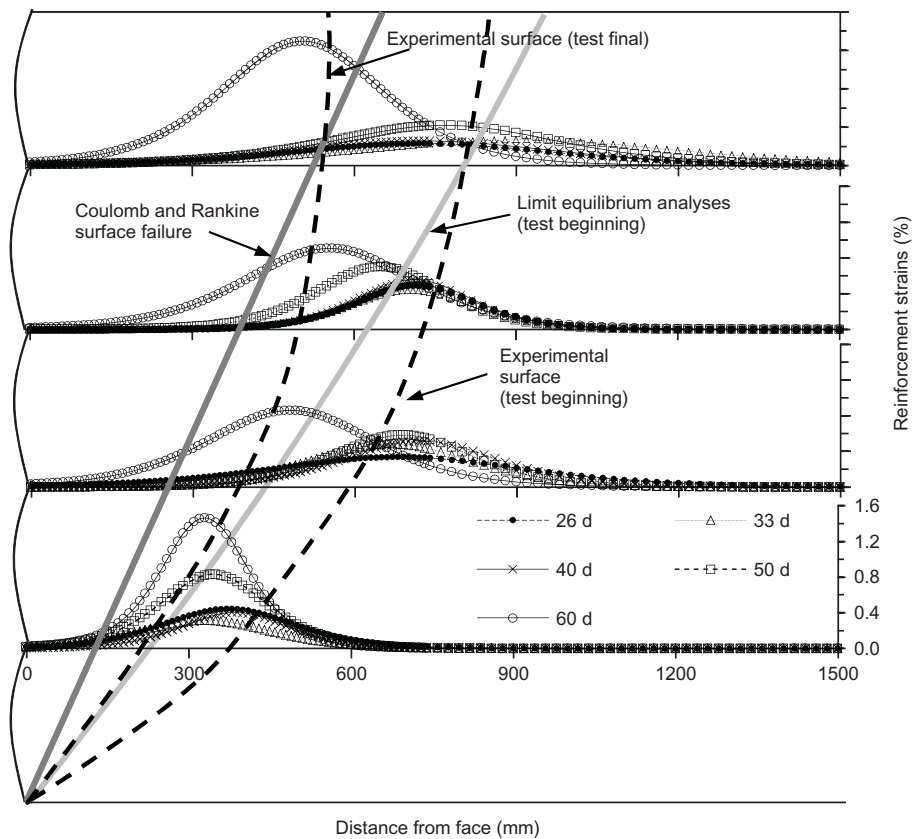


Figure 19. Strain distributions of reinforcements and theoretical surfaces in prototype 1

surface defined using limit equilibrium (including the reinforcement stabilising forces) and the Coulomb failure plane are compared in the figure. The figure shows that the location of peak strains forms a well-defined internal failure plane within the reinforced zone. However, the failure plane predicted using limit equilibrium (considering the friction angle from CD triaxial tests) is deemed accurate for practical purposes. The Coulomb surface is shown to represent the actual potential failure plane less accurately than limit equilibrium. Additionally, peak strains appear to relocate to regions closer to the face during the test. This relocation is associated with the relocation of maximum tension in this reinforcement line due to wetting processes. Figure 19 shows that the relocation is progressive with the wetting advancement.

Figure 20 illustrates the chronology of reinforcement peak strains for prototype 1. The results show strains of up to 0.8% in reinforcement layers 2 and 4, and maximum strains of 1.4% and 1.2% in reinforcement layers 3 and 5. In general, the maximum peak strains were consistent with their given location over the wall height according to Miyata and Bathurst (2007) for geosynthetic-reinforced walls; however, the maximum peak strain in the upper reinforcement layer (layer 5) was higher than expected, which can be attributed to the proximity of the loading system to this reinforced layer.

These results indicate that strains remained generally very small even under combined wetting and sustained loading. The dissipation of pore water pressure through the reinforcement and the enhancement of geotextile mechanical properties due to the influence of soil confine-

ment are assumed to have contributed to keeping the geotextile strains small. The increase in strains with time resulted from the time-dependent advancement of the wetting front, which in turn resulted in progressive decreases in soil stiffness. No positive pore water pressures were detected in the prototype 1 test, which may have influenced the satisfactory displacements observed in this test.

Figure 21 presents the face displacements along the prototype 1 elevation. After five events of rainfall, face displacements reached a value of 2.5 mm. After the rainfall 6 event, face displacements increased substantially as a result of the advancement of wetting to the prototype's toe. The largest face displacement occurred initially in reinforced layer 3 (located at an elevation of 75 cm). As soon as the wetting reached the toe, the largest face displacements occurred in reinforced layer 2 (at an elevation of 45 cm). These results are consistent with those obtained using centrifuge models by Zornberg *et al.* (1998), who reported that the maximum strains for steep slopes occurred towards the mid-height of the structure. A similar behaviour was also observed by Benjamin *et al.* (2007).

4.2. Performance under increasing surcharge: prototype 2

Generally, the greater part of the displacement of geosynthetic-reinforced soil wall occurs during the construction process. Eventually, precipitation can also occur during this period and water pressures can be built up. In order to verify the geotextile's efficiency in dissipation of pore

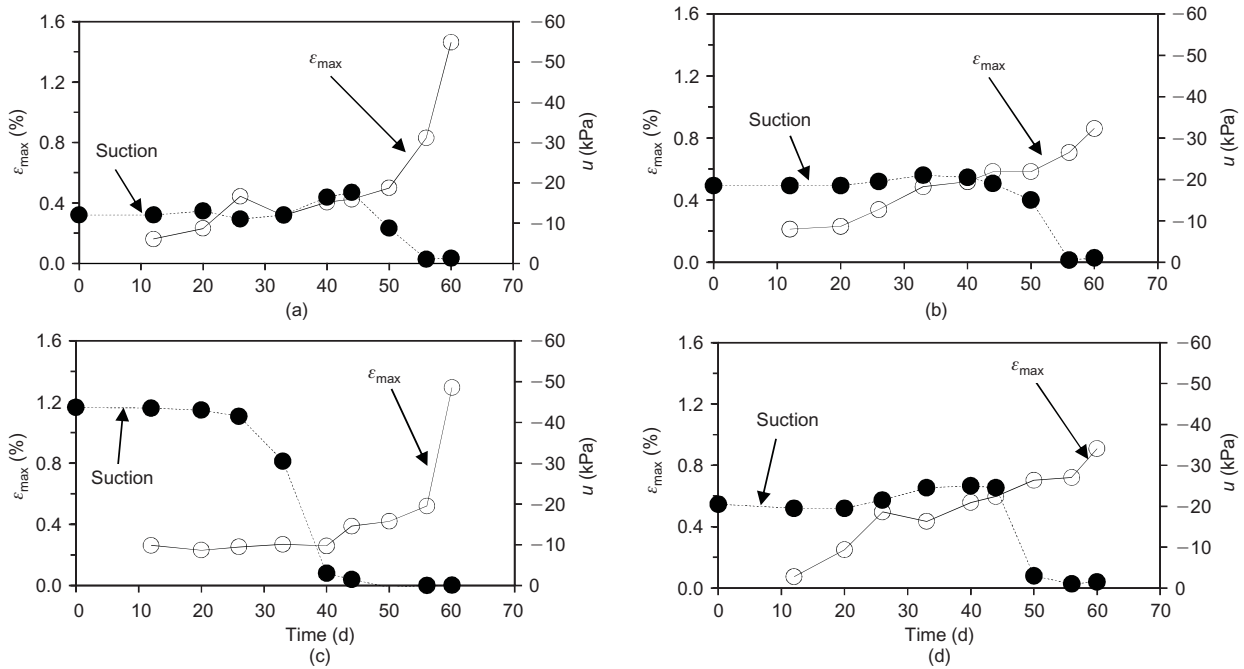


Figure 20. Reinforcement peak strains against time and suction against time in prototype 1: (a) layer 5; (b) layer 4; (c) layer 3; (d) layer 2

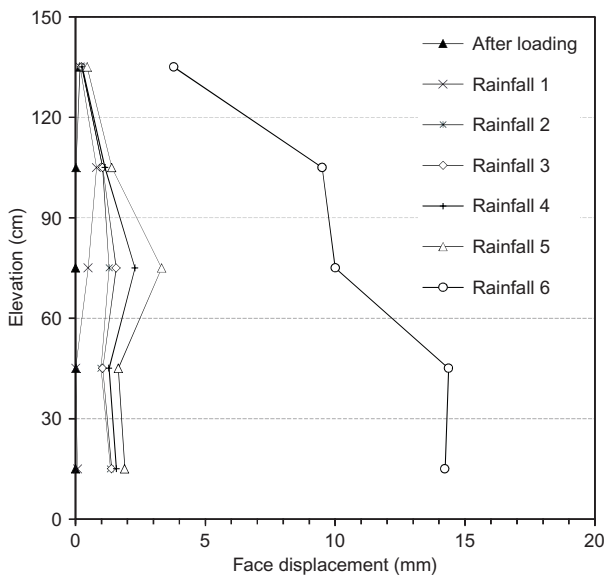


Figure 21. Distribution of face displacement along the prototype 1 elevation

water pressures, this parameter was monitored along reinforcement layer 5 during increasing surcharge (Figure 20). Figure 22a shows that comparatively small pore water pressures were developed after surcharge loadings to 150 and 200 kPa, although they were rapidly dissipated along the reinforcement. Most of the time, pore water pressures remained constant (−5 kPa) even after loading increments. Figure 22b shows pore water pressure results obtained from CU (consolidated undrained) triaxial tests in saturated samples, illustrating the potential for development of pore water pressures in this soil. Therefore, the geotextile is assumed to have provided efficient internal drainage, avoiding excessive pore water pressures even after load increments.

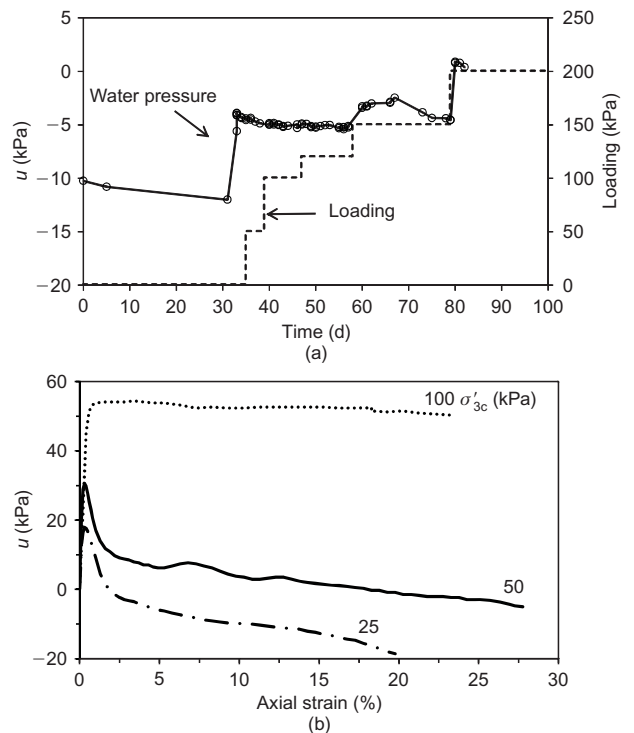


Figure 22. Pore water pressure (u) development: (a) after loading increments in prototype 2; (b) from CU triaxial tests

The effect of increase of loadings on the reinforcement peak strains of the structure evaluated in prototype 2 is illustrated in Figure 23. Clearly, the increments of loading have resulted in increases in the strains, and higher rates of increase are observed to have followed the periods in which the applied loads were higher and the wetting of the soil had been completed. Since significant pore water pressures were not registered, the effect of high levels of loading is assumed to have resulted in this behaviour.

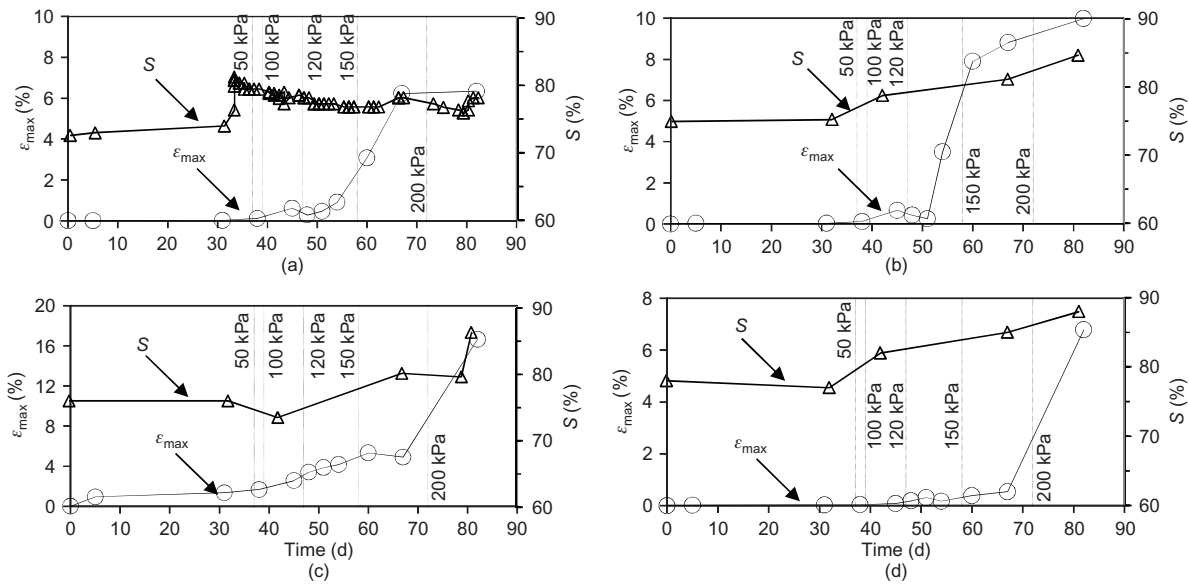


Figure 23. Reinforcement peak strains in prototype 2: (a) layer 5; (b) layer 4; (c) layer 3; (d) layer 2

The data collected in the prototype simulations illustrate the good performance of walls using nonwoven geotextiles under conditions that lead reinforced soils walls to severe serviceability problems. The key for the understanding of the performances reported is around the secondary function of reinforcements (perhaps primary), which is the dissipation of water pressures from the backfill, which improves the geotextile–soil interface strength under wetting conditions. Another aspect is that large deformations are expected for the mobilisation of stresses by nonwoven geotextiles as reinforcements; nevertheless, the research data show very small displacements even after wetting in working conditions.

5. CONSISTENCY OF FIELD AND PROTOTYPE RESPONSES

Common aspects of field performance and prototype simulations were observed in this research. Specifically, wetting of the backfill soil in the case history wall was identified by the field survey conducted in July 2010, 26 years after construction. Although complete wetting of the toe of the structure was not confirmed, there are indications of water infiltration below mid-height of the wall (Figure 6). Water content values measured in the nonwoven geotextile section of the structure were found to be below those observed in the woven geotextile section. Overall, the performance of the nonwoven geotextile section was better than that of the woven geotextile section. The

precipitation data for the highway SP-123 wall (case history) indicates intense rainfall during wall construction. The higher displacements that occurred in the woven geotextile wall are assumed to result from the development of positive water pressures during the construction, which may have not developed in the nonwoven geotextile wall section. In fact, the piezometers installed within the nonwoven geotextile wall did not record positive pore water pressures. Another beneficial effect of the use of nonwoven geotextile is the better interaction with fine-grained soils, in comparison with woven geotextile. Table 1 compares the interface strength of soil–nonwoven geotextile and soil–woven geotextile from shear strength tests conducted by Vidal *et al.* (1990), along with the interface strength between soil and geotextile used in this research. The results in this table show the good interaction properties of nonwoven geotextiles, which can be attributed to the impregnation and penetration of soil particles into the pores of the geotextile. This phenomenon is not expected to occur in woven geotextiles. Under wetting conditions, the interface strength for a woven geotextile and fine soil may be reduced in comparison with a nonwoven geotextile interface (Fabian and Fourie 1986).

The prototype simulations support the field behaviour of the SP-123 wall in different aspects.

- Positive pore water pressures were negligible throughout the entire simulation, even after wetting and loadings increments

Table 1. Soil and interface strength of SP123 wall and full-scale prototype

Structure	Strength parameters	Soil	Soil–nonwoven geotextile	Soil–woven geotextile
SP123 Wall (Vidal <i>et al.</i> 1990)	Cohesion (kPa)	22	15	9
	Friction angle (°)	35	35	35
Full-scale model	Cohesion (kPa)	15	3	–
	Friction angle (°)	32	34	–

- Significant reinforcement strains occurred after loading increments, which is consistent the displacements reported during construction of the SP-123 wall. No significant displacements and reinforcement strains were observed under working stress conditions.
- Reinforcement strains were relatively small, although materials of comparatively low stiffness were used as reinforcements.

Therefore, the relatively high soil stiffness, the drainage capacity of nonwoven geotextiles and the significant interaction between fine-grained soils and geotextiles are relevant for good performance of geotextile-reinforced soil walls. A comparison of reinforcement maximum displacements between field and prototype simulations under working conditions is presented in Figure 24. Similarities of maximum displacements location along the normalised height of field performance and prototypes can be noted.

6. CONCLUSIONS

This paper reports the Brazilian pioneer case of a geotextile-reinforced wall constructed with fine-grained soil. This wall has shown excellent performance since 1986, even after periods of significant precipitation and wetting of the backfill. In order to better assess the adequate performance of this case history structure while providing understanding of the use of nonwoven geotextiles as reinforcement of poor draining soils, prototype full-scale simulations were conducted. Based on the analysis, simulation interpretation and field performance, the following conclusions can be drawn.

- Nonwoven geotextiles have been shown to be useful for reinforcing fine-grained soils, providing internal drainage and good interaction properties.
- The behaviour of the full-scale prototype simulation is consistent with the performance of the case history of the SP-123 wall; data gathered from the full-scale

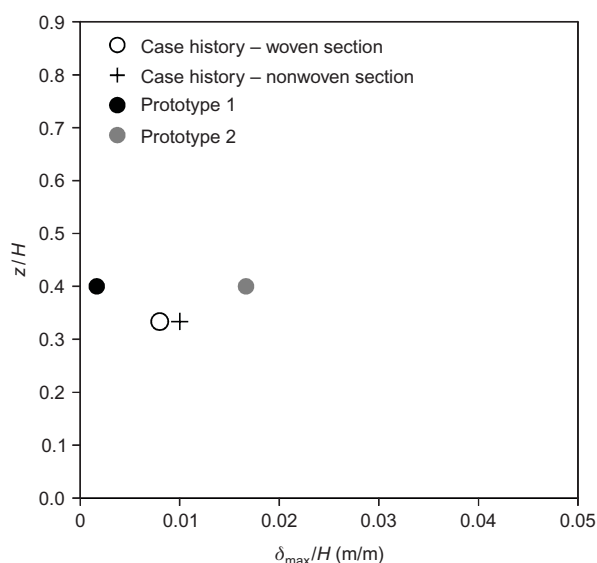


Figure 24. Magnitude and location of reinforcement maximum displacements for the SP-123 wall and full-scale prototype wall under working conditions

prototype showed relatively small horizontal displacements even under comparatively wet conditions.

- Both prototype simulations and field monitoring results showed comparatively high horizontal displacements induced by surcharge loading. The higher displacements observed in this case are attributed to the reduction of soil stiffness induced by soil wetting, associated with high surcharge loading levels. No build-up of pore water pressures induced by rapid loading was observed near the geotextile.
- Positive pore water pressures were not observed to develop with either wetting or loading increments in the prototype simulation. This is attributed to the internal drainage provided by permeable reinforcements.
- The reinforcement peak strains increase progressively with the reduction of matrix suction of soil in each reinforced layer. The rates of increase of strain rises with the advancement of wetting downwards to the prototype's toe.
- Potential failure surface of prototypes approximated to the failure planes from limit equilibrium analyses.
- Although the progressive wetting resulted in increasing displacements and reinforcement strains, they remained relatively small until the wetting front reached the toe of the prototype under working stress conditions. Higher displacements were observed to occur after complete wetting, which can be attributed to the total reduction of fill stiffness.
- Both backfill soils (case history and simulation) showed consistent behaviour in terms of levels of maximum displacements and location of these along the wall height. In addition, the wetting did not significantly affect the performance of nonwoven geotextile walls.

ACKNOWLEDGEMENTS

Special thanks to the State of São Paulo Research Foundation (FAPESP) and the National Council for Scientific and Technological Development of the Brazilian government (CNPq), for financial support of this research. The authors are also grateful to Department of Roadways and Highways of Brazil (DER – Taubaté) for its help in the case history survey.

NOTATION

Basic SI units given in parentheses.

- a, b, c sigmoid regression parameters (dimensionless)
- G_s specific gravity of grains (dimensionless)
- i inclination (degree)
- S degree of saturation (dimensionless)
- u pore water pressures (Pa)
- w water content (dimensionless)
- w_L liquid limit (dimensionless)
- w_{opt} optimum water content from standard Proctor test (dimensionless)

w_p	plasticity limit (dimensionless)
x	relative displacement (m)
ε	reinforcement strains (dimensionless)
ε_{\max}	reinforcement peak strains (dimensionless)

ABBREVIATIONS

AASHTO	American Association of State Highway and Transportation Office
ASTM	American Society for Testing and Materials
CD	consolidated drained
CU	consolidated undrained
FDR	frequency domain reflection
GRS	geosynthetic-reinforced soil
NBR	Brazilian Standards
PI	plasticity index

REFERENCES

- AASHTO (2002). Standard Specifications for Highway Bridges. *American Association of State Highway and Transportation Officials, Div. 1, Sect. 5, Retaining Walls*, 17th edition. AASHTO, Washington, DC, USA, p. 89.
- ASTM D 2937. *Standard Test Method Density of Soil in Place by the Drive-Cylinder Method*. ASTM International, West Conshohocken, PA, USA.
- ASTM D 4595. *Standard Test Method for Tensile Properties of Geotextile by the Wide-width Strip Method*. ASTM International, West Conshohocken, PA, USA.
- Benjamin, C. V., Bueno, B. & Zornberg, J. G. (2007). Field monitoring evaluation of geotextile-reinforced soil retaining wall. *Geosynthetics International*, **14**, No. 2, 100–118.
- BSI (1995). BS 8006. *Code of Practice for Strengthened/reinforced Soils and Other Fills*. BSI, London, UK.
- Carvalho, P. A. S., Pedrosa, J. A. B. A. & Wolle, C. M. (1986). Geotextile reinforced embankment – an alternative to geotechnical engineering. *Proceedings of Brazilian Conference on Soil Mechanics and Foundations*, 8, Porto Alegre, RS, Brazil, October 1986, pp. 169–178 (in Portuguese).
- Ehrlich, M., Vidal, D. & Carvalho, P. A. (1997). Performance of two geotextile reinforced soil slopes. *Proceedings of International Symposium on Recent Developments in Soil and Pavement Mechanics*, Rio de Janeiro, RJ, Brazil, pp. 415–420.
- Elias, V. & Christopher, B. R. (1998). *Mechanically Stabilized Earth Walls and Reinforced Soil Slopes Design and Construction Guidelines*, FHWA-SA-96–071. Federal Highway Administration, Washington, DC, USA.
- Fabian, K. J. & Fourie, A. B. (1986). Performance of geotextile-reinforced clay samples in undrained triaxial tests. *Geotextiles and Geomembranes*, **4**, No. 1, 53–63.
- Fourie, A. B. & Fabian, K. J. (1987). Laboratory determination of clay geotextile interaction. *Geotextiles and Geomembranes*, **6**, No. 4, 275–294.
- Fowze, J. S. M., Bergado, D. T., Soralump, S. & Voottipreux, M. (2012). Rain-triggered landslides hazards and mitigation measures in Thailand: From research to practice. *Geotextiles and Geomembranes*, **30**, No. 1, 50–64.
- França, F. A. N. & Bueno, B. S. (2011). Creep behavior of geosynthetics using confined-accelerated tests. *Geosynthetics International*, **18**, No. 5, 242–254.
- Iryo, T. & Rowe, R. K. (2005). Infiltration into an embankment reinforced by nonwoven geotextiles. *Canadian Geotechnical Journal*, **42**, No. 4, 1145–1159.
- Koerner, R. M. & Soong, T. Y. (2001). Geosynthetic reinforced segmental retaining walls. *Geotextiles and Geomembranes*, **19**, No. 6, 359–386.
- Ling, H. I., Wu, J. T. H. & Tatsuoka, F. (1993). Short-term strength and deformation characteristics of geotextiles under typical operational conditions. *Geotextiles and Geomembranes*, **11**, No. 2, 185–219.
- Mendes, M. J. A. & Palmeira, E. M. (2008). Effects of confinement and impregnation on nonwoven geotextiles mechanical behavior. *Proceedings of Pan American Geosynthetics Conference and Exhibition*, Cancun, Mexico, pp. 540–545.
- Mitchell, J. K. & Zornberg, J. G. (1995). Reinforced soil structures with poorly draining backfills, Part II: Case histories and applications. *Geosynthetics International*, **2**, No. 1, 265–307.
- Miyata, Y. & Bathurst, R. J. (2007). Development of K-stiffness method for geosynthetic reinforced soil walls constructed with $c-\phi$ soils. *Canadian Geotechnical Journal*, **44**, No. 12, 1391–1416.
- NBR 12568. (1992). *Geosynthetics e Determination of Mass Per Unit Area*. Brazilian Association of Technical Standards, Rio de Janeiro, Brazil (in Portuguese).
- NBR 12569. (1992). *Geotextiles e Determination of Thickness*. Brazilian Association of Technical Standards, Rio de Janeiro, Brazil (in Portuguese).
- Noorzad, R. & Mirmoradi, S. H. (2010). Laboratory evaluation of the behavior of geotextile reinforced clay. *Geotextiles and Geomembranes*, **28**, No. 4, 386–392.
- Pathak, Y. P. & Alfaro, M. C. (2010). Wetting–drying behavior of geogrid-reinforced clay under working load conditions. *Geosynthetics International*, **17**, No. 3, 144–156.
- Raisinghani, D. V. & Viswanadham, B. V. S. (2010). Evaluation of permeability characteristics of a geosynthetic-reinforced soil through laboratory tests. *Geotextiles and Geomembranes*, **28**, No. 6, 579–588.
- Raisinghani, D. V. & Viswanadham, B. V. S. (2011). Centrifuge model study on low permeable slope reinforced by hybrid geosynthetics. *Geotextiles and Geomembranes*, **28**, No. 6, 579–588.
- Spencer, E. (1967). A method of analysis of stability of embankments assuming parallel inter-slice forces. *Geotechnique*, **17**, No. 1, 11–26.
- Stulgis, R. P. (2005). Full-scale MSE test walls. *Proceedings of NAGS 2005/GRI-19 Conference*, Las Vegas, NV, USA (CD-ROM).
- Tan, S. A., Chew, S. H., Ng, C. C., Loh, S. L., Karunaratne, G. P. & Delmas Ph Loke, K. H. (2001). Large-scale drainage behavior of composite geotextile and geogrid in residual soil. *Geotextiles and Geomembranes*, **19**, No. 3, 163–176.
- Tatsuoka, F. & Yamauchi, H. (1986). A reinforcing method for steep clay slopes using a non-woven geotextile. *Geotextiles and Geomembranes*, **4**, No. 3, 241–268.
- Vidal, D., Carvalho, P. A. S., Ehrlich, M. & Silvia, L. F. M. (1990). Analysis of a reinforced soil structure through laboratory tests and field instrumentation. *Proceedings of Brazilian Conference on Soil Mechanics and Foundations*, Salvador, Bahia, Brazil, Vol. 1, pp. 35–37.
- Wright, S. G. & Duncan, J. M. (1991). Limit equilibrium stability analyses for reinforced slopes. *Transportation Research Record*, **1330**, 40–46.
- Yoo, C. & Jung, H. Y. (2006). Case history of geosynthetic reinforced segmental retaining wall failure. *Journal of Geotechnical and Geoenvironmental Engineering, ASCE*, **132**, No. 12, 1538–1548.
- Zornberg, J. G. & Mitchell, J. K. (1994). Reinforced soil structures with poorly draining backfills, Part I. *Geosynthetics International*, **1**, No. 2, 103–148.
- Zornberg, J. G. & Arriaga, F. (2003). Strain distribution within geosynthetic-reinforced slopes. *Journal of Geotechnical and Geoenvironmental Engineering*, **129**, No. 1, 32–45.
- Zornberg, J. G., Sitar, N. & Mitchell, J. K. (1998). Performance of geosynthetic reinforced slopes at failure. *Journal of Geotechnical and Geoenvironmental Engineering*, **124**, No. 8, 670–683.

The Editor welcomes discussion on all papers published in *Geosynthetics International*. Please email your contribution to discussion@geosynthetics-international.com by 15 October 2013.